Available online at www.sciencedirect.com
ScienceDirect
Lithos 96 (2007) 55–66
LITHOS
www.elsevier.com/locate/lithos

Chemical and stable isotopic constraints on the nature and origin of volatiles in the sub-continental lithospheric mantle beneath eastern China

Mingjie Zhang [a,*], Peiqing Hu [a], Yaoling Niu [b,c], Shangguo Su [c]

[a] Key Lab of Western China's Environmental Systems (MOE), Lanzhou University, Gansu 730000, China
[b] Department of Earth Sciences, Durham University, Durham DH1 3LE, UK
[c] China University of Geosciences, Beijing 100083, China

Received 31 March 2006; received in revised form 13 September 2006; accepted 24 October 2006
Available online 17 January 2007

Abstract

We report concentrations and stable isotopic data of CO_2, CO, CH_4, H_2O and H_2 volatile species from mantle xenoliths hosted in Cenozoic basalts in eastern China. The volatiles are extracted by stepwise heating and mostly released in two temperature intervals, ~400–600 °C and ~800–1200 °C, respectively. We identified two types of volatiles: (1) "initial" volatiles, which were originally dissolved in crystal structures and trapped in fluid inclusions in the interiors of mineral crystals, are released at the 800–1200 °C interval, and composed of H_2 (66.6 mm^3.STP/g on average), CO_2 (50.7), CO (35.8) and CH_4 (0.6). The δD and $\delta^{13}C$ of CH_4 exhibit "normal" mantle signatures. However, variable $\delta^{18}O$ of CO_2 (0.6‰ to 16.6‰) and lighter $\delta^{13}C$ values of CO_2 and CO point to the involvement of a recycled crustal component. We interpret the latter as subducted oceanic crust with terrigenous sediments. (2) metasomatic volatiles, which were incorporated into minerals as fluid inclusions at edges and healed fractures of the recrystallizing minerals probably during mantle metasomatism, are released at the 400–600 °C interval, and composed mainly of CO_2 (~9.82 mm^3.STP/g on average) with minor CO, H_2 and CH_4, and are characterized by $\delta^{13}C$ of biogenic CH_4, lighter and variable δD of H_2O (−110.7‰ to −280.9‰), lighter $\delta^{13}C$ of CO_2 and CO and variable $\delta^{18}O$ of CO_2 (1.0‰ to 11.5‰), suggesting that the metasomatic volatiles may have originated form devolatilization of altered recycled oceanic crust with terrigenous sediments. We speculate that the metasomatic volatiles could have come from dehydration of the subducted paleo-Pacific lithosphere that lies horizontally in the transition zone beneath eastern China. Such recycled crustal fluids may have been important in metasomatizing the sub-continental lithosphere beneath eastern China and in causing thinning of the lithosphere and associated magmatism in the Mesozoic.
© 2006 Elsevier B.V. All rights reserved.

Keywords: Origin of volatile; Concentration; Stable isotope; Lherzolite xenoliths; Sub-continental lithospheric mantle; Eastern China

1. Introduction

Volatiles in the Earth's mantle are a mixture of volatiles trapped during Earth formation and volatiles recycled from the atmosphere, hydrosphere and crustal materials into the mantle by subduction. The recycled

* Corresponding author. Institute of Geological Science, Lanzhou University. Tel.: +86 931 8912403; fax: +86 931 8912449.
E-mail address: mjzhang@lzu.edu.cn (M. Zhang).

0024-4937/$ - see front matter © 2006 Elsevier B.V. All rights reserved.
doi:10.1016/j.lithos.2006.10.006

volatiles are likely to have diverse identities because of their different origins and complex histories. Consequently, the abundances, types and characteristics of volatile species and their isotopic compositions in mantle materials can be used to decipher their ultimate origins and passageways in the context of crust-mantle recycling and mantle circulation. Indeed, studies in this area have proven to be promising (e.g., Harmon et al., 1986/87; Woodhead et al., 1993; Trull et al., 1993; Ionov et al., 1994; Harmon and Hoefs, 1995; Eiler et al., 1995; Hansteen and Troll, 2003; Widom and Farquhar, 2003; Demeny et al., 2004; Shaw et al., 2004; Schulze et al., 2004).

Carbon isotopic composition varies significantly in natural carboniferous phases. For example, the $\delta^{13}C$ of biogenic methane varies from −66.1‰ to −69.2‰ (Schoell, 1988; Xia and Wang, 1996; Avery and Martens, 1999). The $\delta^{13}C$ of organic matters in sediments is about −25‰, and the $\delta^{13}C$ of ~−5‰ has been identified as a characteristic value of mantle materials, e.g., kimberlite, mantle xenoliths and fresh glasses of mid-ocean ridge basalts (MORB) and ocean island basalts (OIB) (Mattey et al., 1984; Exley et al., 1986; Deines, 2002). The $\delta^{13}C$ of diamonds varies from −27.9‰ to −3.2‰ (Deines et al., 1997). The $\delta^{13}C$ of mantle xenoliths are from −30‰ to 0‰ with bimodal peaks at −5‰ (at releasing temperature >900 °C) and −25‰ (<900 °C) respectively (Nadeau et al., 1990; Pineau and Mathez, 1990; Trull et al., 1993; Deines, 2002). The ^{13}C depletion is interpreted as carbon mass fractionation of an isotopically homogeneous mantle in the presence of a C–O–H fluid phase or a ^{12}C-rich mantle component (Deines et al., 1997; Shaw et al., 2004), graphitic or organic materials (Exley et al., 1986; Pineau and Mathez, 1990; Nadeau et al., 1990) or recycled crustal components (Trull et al., 1993; Schulze et al., 2004). Nevertheless, the bimodal distribution remains poorly understood (Deines, 2002), and more data are needed to assess these notions.

The $\delta^{18}O$ values of terrigenous sediments vary from +15‰ to +25‰ (Eiler et al., 1995, 1997). "Normal" mantle is widely accepted to have $\delta^{18}O$ values of ~+5.5‰ (Kyser, 1986; Mattey et al., 1994) and δD values of −40‰ to −95‰ (a mean of −80‰, Boettcher and O'Neil, 1980; Kyser and O'Neil, 1984; Kyser, 1986). These mantle $\delta^{18}O$ values are acquired from oceanic gabbros (+3.3‰ to +5.1‰, Hansteen and Troll, 2003), fresh MORB/OIB glasses (+5.7‰ to +6.0‰, Eiler et al., 1996, 1997; Widom and Farquhar, 2003) and olivines in mantle xenoliths and of MORB phenocrysts (+5.2‰ on average, Mattey et al., 1994; Eiler et al., 1997). Mantle spinel and garnet lherzolites have relatively uniform $\delta^{18}O$ (+4‰ to +7‰; Kyser et al., 1982; Harmon et al., 1986/87; Ionov et al., 1994). Lighter $\delta^{18}O$ values have been interpreted as contributions from recycled altered oceanic crust or interaction with seawater (Lowry et al., 1999; Macpherson et al., 2000; Widom and Farquhar, 2003), and heavier $\delta^{18}O$ values (+14.1 to +16.4‰) are thought to be terrigenous sediments (MacGregor and Manton, 1989; Hansteen and Troll, 2003). Strong negative δD shift is caused by the devolatilization of crustal rocks (Ripley et al., 1992).

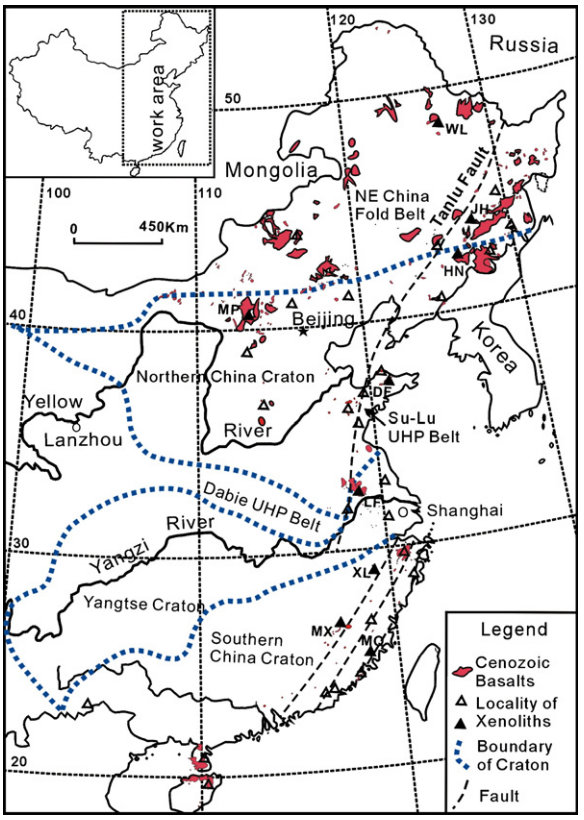


Fig. 1. Sample locations for lherzolite xenoliths in eastern China, Modified after those of Fan and Hooper (1989) and Tatsumoto et al. (1992). Location of sampled xenolith is indicated by a filled triangle with a locality abbreviation, such as WL — Wudalianchi; JH — Jiaohe, HN — Huinan; MP — Damaping, DF — Dafangshan, LF — Liuhefangshan; XL — Xilong; MQ — Mingqing and MX — Mingxi.

Combined studies of C, O and H isotopes and concentrations of volatiles in mantle xenoliths should allow faithful identification of various source components in the volatiles. For example, a detailed stable isotope study of diamonds from the Jwaneng kimberlite reveals at least seven physically or chemically distinct formation environments (Deines et al., 1997). However, very few combined stable isotope and concentration studies

yet exist on volatiles in mantle xenoliths mostly because of the paucity of volatiles in such rocks and constituent minerals, thus technically difficult to study the relevant isotopes (Xia et al., 2004). Consequently, we know very little about C, O and H isotope compositions and concentration levels of CO_2, CO, CH_4, H_2O and H_2 in mantle materials proper.

In this paper, we present for the first time the C, O and H isotopic compositions and concentrations of CO_2, CO, CH_4, H_2O and H_2 from bulk-rock and mineral separates of mantle lherzolite xenoliths hosted in Cenozoic basalts from eastern China. These new data provide insights into the origin of volatiles from the subcontinental lithospheric mantle (SCLM) in the context of crust-mantle recycling, and new perspectives on the lithosphere thinning beneath eastern China and intraplate volcanism away from plate boundaries.

2. Samples and analytical procedure

In this study, we collected fresh spinel lherzolite xenoliths from Wudalianchi (WL), Jiaohe (JH), Huinan (HN), Damaping (MP), Dafangshan (DF), Liuhefangshan (LF) and Mingqing (MQ); spinel and garnet lherzolite from Xilong (XL); and garnet lherzolite xenoliths from Mingxi (MX) in eastern China (Fig. 1). The samples were crushed to ~0.2–0.9 mm. Olivine (Oliv), orthopyroxene (Opx) and clinopyroxene (Cpx) separates of >99% purity were hand-picked under a binocular microscope to remove altered fragments. Mineral separates and bulk-rock lherzolite xenoliths (Lht) were then (1) ultrasonically cleaned with 0.3 mol/L HCl and analytically pure CH_2Cl_2 respectively to remove possible carbonate and organic contaminants, (2) rinsed with distilled water at each step until pH value reaches around 7, and (3) dried in an oven at 110 °C.

The well-established stepwise-heating volatile extraction method combining mass-spectrometry is routinely used for concentration and isotope analysis of volatiles in mantle xenoliths (Nadeau et al., 1990; Pineau and Mathez, 1990; Zhang et al., 2004, 2005). An ameliorative online vacuum stepwise-heating mass spectrometer was used to determine chemical compositions of the volatiles in mineral separates and bulk-rock samples. The volatile extraction apparatus has a quartz sample tube and a cold trap, and is directly connected to MAT-271 mass spectrometer. Each sample is loaded in the quartz tube and heated for 1 h under high-purity O_2 at 200 °C to remove the residual surface organic matter. The volatiles potentially adsorbed on mineral surface and in cracked inclusions were degassed in a vacuum of 1×10^{-3} Pa for 4 h before being stepwise heated from 300 °C to 1200 °C at 100 °C steps. The temperature at each step is held for 1 h, and a cold trap with liquid nitrogen is used to condense and isolate H_2O, CO_2 volatiles from high temperature area to prevent reactions with other released gases. Then, all volatiles (except for H_2O) are released using an cold trap with alcohol-liquid nitrogen mixture and introduced to the MAT 271 mass spectrometer for volatile concentration measurement. The standard deviations are typically <1 mol% for CO_2, CO and H_2 etc.

Carbon isotopes of CO_2, CO and CH_4, which is expressed as $\delta^{13}C\ (‰)=([^{13}C/^{12}C]_{sample}/\ [^{13}C/^{12}C]_{PDB}-1)\times10^3$ (where PDB, Pee Dee Belemnite, is the reference standard), were analyzed by a GC-C-MS system using a stepwise-heating extraction procedure. The volatile extraction apparatus, which has a quartz sample tube, a cold trap and a molecular sieve trap, is directly connected to the GC-C-MS system. Each sample is loaded into the sample tube, and degassed in helium carrier gas at 200 °C for 4 h to remove potentially surface-adsorbed gases; meanwhile the molecular sieve is activated at 400 °C. The sample is then heated from 400 °C to 1200 °C at 200 °C steps held for 1 h at each step. The released volatiles are collected with the molecular sieve tube using liquid nitrogen cooling method. The volatiles were then released by heating after each step and introduced into the GC-C-MS system by helium carrier gas. The CO_2, CO and CH_4 are separated by an Agilent 6890N gas chromatographic analyzer through a 4 m long GDX-05 packed-stainless steel column with helium carrier gas at a flow rate of 5 cm^3/min. The column temperature is initially set at −20 °C, and is increased at 3 °C/min from −20 °C to 95 °C. The separated components were subsequently combusted into CO_2 and sent into a Delta plus XP mass spectrometer for carbon isotope analysis. The reported $\delta^{13}C$ (relative to VPDB) values have a relative error of ±0.2‰.

Oxygen isotopic composition is expressed as $\delta^{18}O\ (‰)=([^{18}O/^{16}O]_{sample}/\ [^{18}O/^{16}O]_{SMOW}-1)\times10^3$ (where SMOW, Standard Mean Ocean Water, is the reference standard), and hydrogen isotopic composition is defined as $\delta D\ (‰)=([D/H]_{sample}/\ [D/H]_{SMOW}-1)\times10^3$. Hydrogen isotopes of H_2O and H_2, and oxygen and also carbon isotopes of CO_2 are analyzed by the vacuum stepwise-heating method using MAT251 and MAT252 mass spectrometers. The volatile extraction apparatus has a quartz sample tube, two cold traps and a CuO oven, and is connected to a pump by a valve. Each sample is loaded into the sample tube, outgassed in a vacuum of 1×10^{-3} Pa at 100 °C for 4 h to remove

Table 1
Volatile concentrations and carbon and oxygen isotopes of CO_2, CO and hydrogen isotopes of H_2O and H_2 of bulk-rock (Lht), olivine (Oliv), orthopyroxene (Opx) and clinopyroxene (Cpx) separates in lherzolite xenoliths of eastern China

Sample	Rock	Mineral	T (°C)	Content (mm^3.STP/g)				$\delta^{13}C$ (‰ vs. PDB)			$\delta^{18}O$, δD (‰ vs. SMOW)		
				CO_2	CO	CH_4	H_2	$\delta^{13}C_{CO2}$	$\delta^{13}C_{CO}$	$\delta^{13}C_{CH4}$	$\delta^{18}O_{CO2}$	δD_{H2O}	δD_{H2}
WL20	sp–lht	Lht	600	4.5	1.65	0.25	1.53	−25.0	−31.0	−36.0			
			800	3.23	4.35	0.20	17.78	−23.0					
			1200	3.03	0.25	0.00	0.95						
LF20	sp–lht	Lht	600	17.54	1.8	0.49	0.17	−33.0	−23.0				
			800	18.11	0	0.03	0.10	−29.0	−26.0				
			1200	6.55	0	0.00	0.02	−19.0					
XL20	sp–gt–lht	Lht	600	2.27	0.54	0.16	0.45	−25.0	−16.0	−34.0			
			800	18.02	1.63	0.43	3.75	−26.0	−28.0				
			1200	4.16	0.06	0.00	0.48	−19.0	−24.0				
MQ20	sp–lht	Lht	600	26.83	0.83	0.66	0.15	−26.0	−3.0	−37.0			
			800	16.68	1.18	0.28	0.45	−28.0	−7.0	−32.0			
			1200	2.89	0	0.00	0.04	−20.0					
JH01	sp–lht	Oliv	400	1.55	0.28	0.05	0.19	−27.0	−17.0		6.2		
			600	2.28	0.21	0.09	0.09	−28.0	−20.0		4.0	−112.2	
			800	2.12	0.02	0.06	0.09	−23.0	−34.0		5.2		
			1000	1.58	0.04	0.02	0.26	−25.4	−29.0		4.7		
			1200	0.29	0.1	0.40	0.40	−23.2	−23.0		4.9	−88.2	
HN01	sp–lht	Oliv	400	1.26	0.28	0.04	0.06	−22.4			1.4		
			600	2.66	0.44	0.05	0.01	−21.0	−27.0		11.0		
			800	1.30	0.91	0.13	0.83	−20.1			4.6		
			1000	0.13	0.24	0.02	0.42	−23.4			7.6		
			1200	0.09	0.27	0.00	0.74	−25.0			2.0		
MP01	sp–lht	Oliv	400	4.05	1.5	0.03	0.05	−23.7			10.2		
			600	0.76	1.28	0.13	0.19	−26.8	−22.9	−33.8	7.6	−111.1	−47.6
			800	0.31	4.42	0.02	0.69	−27.7	−22.6	−27.1			
			1000	0.31	3.49	0.00	0.11	−26.6					
			1200	0.16	1.02	0.00	0.08	−17.6	−25.3	−28.1	8.2	−48.7	−73.8
DF01	sp−lht	Oliv	400	1.21	1.08	0.14	0.09	−29.0	−24.0		13.3		
			600	1.91	1.71	0.24	0.37	−28.0	−33.0		8.3	−210.3	
			800	3.22	6.21	0.09	0.76	−22.0		−39.0	6.7		
			1000	0.64	7.21	0.00	0.56	−23.0	−28.0		7.5		
			1200	0.45	2.7	0.00	0.01	−21.0	−26.0		6.5		
MX01	gt–lht	Oliv	400	0.51	0.11	0.04	0.03	−29.0	−28.0	−56.0	11.5		
			600	0.95	0.36	0.08	0.01	−28.0	−15.0	−53.0	7.3	−118.8	
			800	1.54	0.92	0.05	0.06	−24.0	−15.0		16.6		
			1000	0.29	0.15	0.04	0.00	−27.0	−27.0		11.7		
			1200	0.26	0.01	0.00	0.00	−21.0	−22.0		2.5		
JH02	sp–lht	Opx	400	1.95	0.86	0.13	0.33	−20.7	−25.0		1.9		
			600	3.77	1.68	0.57	3.69	−24.1	−30.0		1.2	−110.7	
			800	5.75	5.64	0.33	53.61	−19.0	−27.0		0.6		
			1000	0.64	2.52	0.06	24.44	−22.9	−36.0		10.1		
			1200	1.40	0.79	0.00	1.48	−29.1	−29.0		13.6	−82.1	
HN02	sp–lht	Opx	400	2.40	0.65	0.10	0.02	−20.9		−48.0	4.8		
			600	3.69	1.86	0.20	0.15	−28.0	−22.0	−47.0	11.1		
			800	1.73	12.12	0.54	27.78	−23.0	−28.0		3.1		
			1000	0.17	7.4	0.21	38.72	−20.7	−27.0		9.9		
			1200	0.03	2.2	0.00	24.01	−29.1	−31.0		8.9		
MP02	sp–lht	Opx	400	7.49	5.38	0.13	0.24	−25.8			1.0		
			600	11.57	6.24	0.40	0.06	−22.5	−26.2	−37.2	10.5	−148.6	−33.8
			800	8.83	14.04	0.23	2.71	−27.4	−29.0	−26.4	11.8		
			1000	1.57	14.79	0.00	4.15	−27.8	−28.0		11.0		
			1200	0.69	4.57	0.00	0.14	−28.5	−27.5	−25.0	6.1	−96.4	−86.4
DF02	sp–lht	Opx	600	1.82	7.59	0.18	3.55	−26.3			5.7	−280.9	
			1200	4.91	35.75	0.37	88.35	−22.1			6.9		
MX02	gt–lht	Opx	400	1.97	0.97	0.12	0.73	−23.2	−25.0		10.1		

Table 1 (*continued*)

Sample	Rock	Mineral	T (°C)	Content (mm^3.STP/g)				$\delta^{13}C$ (‰ vs. PDB)			$\delta^{18}O$, δD (‰ vs. SMOW)		
				CO_2	CO	CH_4	H_2	$\delta^{13}C_{CO2}$	$\delta^{13}C_{CO}$	$\delta^{13}C_{CH4}$	$\delta^{18}O_{CO2}$	δD_{H2O}	δD_{H2}
			600	2.42	1.75	0.25	0.79	−22.3	−32.0		5.6		
			800	1.26	6.21	0.46	60.76	−18.0	−28.0				
			1000	0.09	7.01	0.03	64.96	−26.7	−29.0		3.5		
			1200	0.18	4.64	0.01	19.38	−25.0	−21.0		6.9	−31.1	
JH03	sp–lht	Cpx	400	1.83	0.24	0.31	0.33	−28.0	−25.0	−53.0			
			600	6.96	1.92	1.18	3.13	−31.0	−30.0	−42.0			
			800	78.1	52.27	0.77	69.3	−27.0	−27.0	−38.0			
			1000	81.09	74.77	0.06	77.89	−28.0	−29.0				
			1200	15.46	3.22	0.03	12.47	−15.0	−37.0				
MP03	sp–lht	Cpx	400	12.75	1.57	0.25	0.12	−27.0	−29.0		5.2		
			600	13.47	1.12	0.94	1.82	−28.0	−22.4	−27.2	3.7	−116.5	−137.1
			800	53.00	8.52	0.19	13.65	−23.0	−28.0	−26.4	0.8		
			1000	37.92	7.37	0.00	21.97		−47.0	−23.6	2.9		
			1200	20.27	3.97	0.00	0.36	−27.0	−28.0	−23.6	8.7	−70.8	−46.1

sp–lht: spinel lherzolite xenolith, gt–lht: garnet lherzolite xenolith, sp–gt–lht: spinel and garnet lherzolite, STP — standard temperature and pressure; PDB — international reference standard of carbon isotope, cretaceous belemnite guard from the Pee Dee Formation in South Carolina, SMOW — international reference standards of oxygen and hydrogen isotopes, standard mean ocean water.

volatiles potentially adsorbed on mineral surfaces and in cracked inclusions, and then heated from 400 °C to 1200 °C at 200 °C steps held for 1 h at each step. The released gases are introduced to the first cold trap with liquid nitrogen to fix the CO_2, H_2O and alkane hydrocarbon etc. The non-condensible gases, mostly CO and H_2, were converted into CO_2 and H_2O by reacting with CuO at 800 °C and fixed into 2nd cold trap by liquid nitrogen cooling. The CO_2 released from the sample is collected in the sample tube by cooling method and measured for carbon and oxygen isotopes using MAT-252 mass spectroscopy. The error is ~±0.2‰ for both $\delta^{18}O$ (relative to VSMOW) and $\delta^{13}C$ (relative to VPDB) values. The $\delta^{13}C$ values of CO_2 so analyzed are close to the results by GC-C-MS system. The H_2O released from the sample and H_2O converted from H_2 at the 400–600 °C and 800–1200 °C intervals were collected respectively into a glass tube filled with metal Zn by cooling method, and reduced to H_2 by reaction with hot zinc metal at 460 °C. The hydrogen isotope is analyzed using MAT-251 mass spectroscopy, and the reported δD values (relative to VSMOW) have an error of ±2‰.

3. Results

The analytical data for CO_2, CO, CH_4 and H_2 concentrations and $\delta^{13}C$, $\delta^{18}O$ and δD values are given in Table 1, where the reported concentrations of CO_2, CO, CH_4 and H_2 are sums of the two sequential steps, e.g., the datum at 400 °C is a summation of data at 300 °C and 400 °C.

3.1. Concentrations of CO_2, CO, CH_4 and H_2

Volatile concentrations in the lherzolite xenolith samples vary considerably, depending on volatile species, mineral phases and releasing temperatures. H_2 is the most abundant with a mean of 40.82 mm^3.STP/g; CH_4 is the least abundant with a mean of 0.77 mm^3.STP/g; CO_2 is most variable, ranging from 3.55 to 183.44 mm^3.STP/g. Concentrations of CO_2, CO, CH_4 and H_2 generally increase from Oliv, Opx to Cpx. Oliv has the lowest CO_2, CO, CH_4 and H_2 contents with a mean of 5.96, 6.99, 0.34 and 1.22 mm^3.STP/g, respectively. Cpx has the highest CO_2 CO, CH_4 and H_2 contents with a mean of 160.43, 77.49, 1.87 and 100.52 mm^3.STP/g, respectively (Table 1).

With stepwise heating, volatiles from bulk-rock samples, and Oliv, Opx and Cpx mineral separates of lherzolite are released progressively with most volatiles

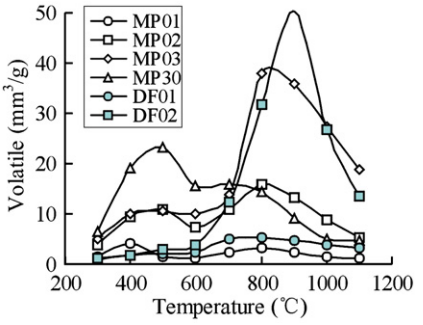


Fig. 2. Plot of volatile contents (excluding H_2O, mm^3.STP/g) in the constituent minerals of lherzolite xenoliths vs. releasing temperature.

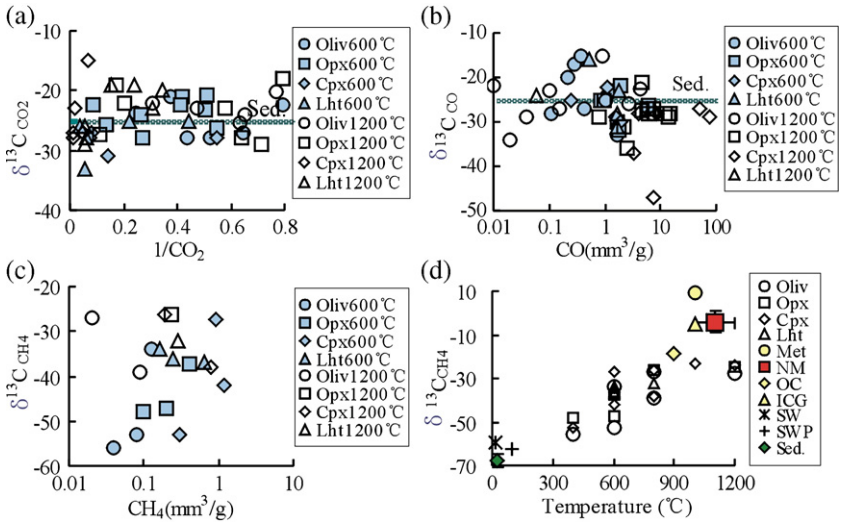


Fig. 3. Plots showing variations of $\delta^{13}C$ (‰ vs. PDB) of CO_2, CO and CH_4 as a function of volatile contents (mm^3.STP/g) and heating temperature (°C); a, b and c plot $\delta^{13}C$ of CO_2, CO and CH_4 vs. their contents; d plots $\delta^{13}C$ of CH_4 vs. heating temperature. Oliv — olivine; Opx — orthopyroxene; Cpx — clinopyroxene in lherzolite xenoliths, Lht — bulk rock of lherzolite xenoliths; 600 °C — refer to temperature of 400 °C and 600 °C, 1200 °C — refer to temperature of 800 °C, 1000 °C and 1200 °C, i.e., values at 400 and 600 °C denoted as 600 °C, and values at 800, 1000 and 1200 °C denoted as 1200 °C; Sed. — sedimentary organic matters (Eiler et al., 1997; Avery and Martens, 1999; Deines, 2002), NM — "normal" mantle (Boettcher and O'Neil, 1980; Kyser and O'Neil, 1984; Kyser, 1986; Schoell, 1988; Mattey et al., 1994), Met — the Murchison meteorite (Yuen et al., 1984), OC — the olivine of oceanic lower crustal gabbros (Kelley and Frueh-Green, 1995), ICG — the inclusion of alkaline Ilimaussq complex, south Greenland (Konnerup-Madsen et al., 1988), SWP — the swamp in NW Germany (Schoell, 1988), SW — the Pacific ocean water (Xia and Wang, 1996).

released at two temperature intervals corresponding to 400–600 °C and 800–1200 °C respectively (Fig. 2; also see Zhang et al., 2004). Variably higher amounts of volatiles are released at the 800–1200 °C interval than at the 400–600 °C interval (Fig. 2). Volatiles released at the 400–600 °C interval are dominated by CO_2 (a mean of ~9.63 mm^3.STP/g). The type and amount of volatiles released at the 800–1200 °C interval depend on mineral phases. Volatiles released at the 800–1200 °C interval are mostly CO (a mean of 5.54 mm^3.STP/g) in Oliv, mostly H_2 (~94.91) with minor CO (~26.82) and CO_2 (~6.74) in Opx, and are dominated by CO_2 (~142.92) and H_2 (~103.88) plus some CO (~75.06) in Cpx (See Table 1 for details).

3.2. Carbon isotopic compositions

CO_2, CO and CH_4 of lherzolite xenoliths have a large range in carbon isotopic compositions, depending on carboniferous species, releasing temperatures and host mineral phases (Fig. 3a, b and c). The $\delta^{13}C$ values of CO_2 vary from −33.0‰ to −15.0‰ with a mode of ~−28.0‰; the $\delta^{13}C$ values of CO range from −47.0‰ to −3.0‰ with a mean of −25.9‰, and CH_4 shows lighter

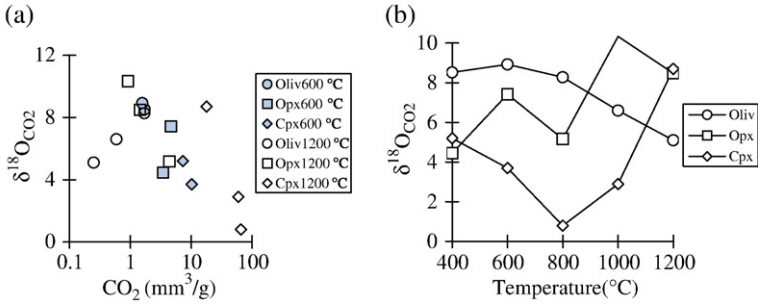


Fig. 4. Plots of average $\delta^{18}O$ values (‰ vs SMOW) of CO_2 vs. average contents of CO_2 (mm^3.STP/g) at each heating temperature (a) and heating temperature (b).

and a large range of $\delta^{13}C$ value from −56.0‰ to −23.6‰. The $\delta^{13}C$ values of CO_2 and CO are ^{13}C-depleted and fall far outside the accepted mantle range (Deines, 2002) and fall into the field of sedimentary organic matters (Fig. 3a, b). The CH_4 displays a conspicuous $\delta^{13}C$ increase with increasing releasing temperature towards mantle values (Fig. 3d). In general, the $\delta^{13}C$ values of CH_4 released at 400–600 °C become lighter with decreasing releasing temperature and CH_4 content, pointing to methane of biogenic origin (Fig. 3c, d).

3.3. Oxygen and hydrogen isotopic compositions

Given that $^{18}O/^{16}O$ fractionation at mantle temperatures is insignificant (e.g., <1‰) (Taylor, 1986), we infer that oxygen isotopes of CO_2 in fluid inclusions also represent those of the coexisting H_2O (despite the possible disequilibrium of oxygen isotopes with the host silicate minerals) (Brady, 1995). The $\delta^{18}O$ values of CO_2 (hence, also H_2O) vary considerably from +0.6‰ to +16.6‰ relative to $\delta^{18}O$ values of lherzolite elsewhere (Kyser et al., 1982; Harmon et al., 1986/87; Ionov et al., 1994). The $\delta^{18}O$ values of CO_2 released at the 400–600 °C interval vary in a smaller range (i.e., 1.0‰ to 11.5‰) than those released at the 800–1200 °C peak (i.e., 0.6‰ to 16.6‰). The average $\delta^{18}O$ values of CO_2 released from Oliv, Opx and Cpx at each releasing temperature are plotted against average CO_2 contents and releasing temperature in Fig. 4. The average $\delta^{18}O$ values of CO_2 in Oliv show a small and scattered positive trend with CO_2 content (Fig. 4a) and a weak decrease with increasing temperature (Fig. 4b). Both $\delta^{18}O$ and $\delta^{13}C$ of CO_2 suggest that the CO_2 may have derived from recycled oceanic crust with sedimentary organic matters (Fig. 5a).

Hydrogen isotopes determined from released H_2O and H_2 show a huge range in terms of δD values (from −31.1‰ to −280.9‰, Table 1). The H_2O seems to have two distinct δD populations. H_2O released at the 800–1200 °C interval shows a small δD range (−31.1‰ to −96.4‰) and fall in the mantle δD field (Boettcher and O'Neil, 1980; Kyser and O'Neil, 1984; Kyser, 1986), whereas H_2O released at the 400–600 °C interval has variably large negative δD values (−110.7‰ to −280.9‰) (Fig. 5b). The δD values of H_2 range from −33.8‰ to −137.1‰, overlapping the mantle δD values (Fig. 5c). The δD of H_2 released at the 400–600 °C interval shows a positive trend with $\delta^{18}O$ of CO_2 (Fig. 5c) and a negative trend with H_2 contents (Fig. 5d).

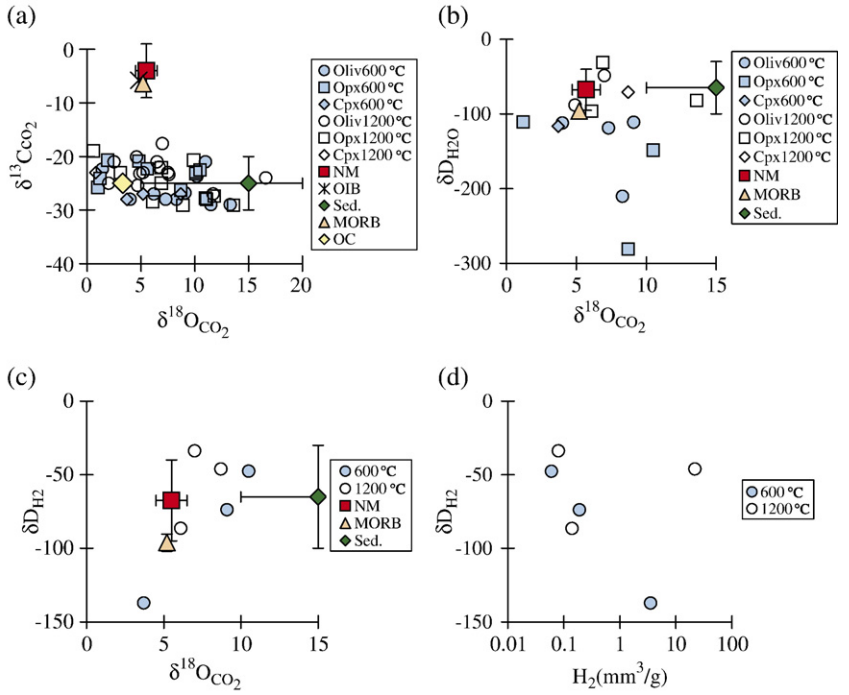


Fig. 5. Relationships among the carbon ($\delta^{13}C$, ‰ vs PDB), oxygen ($\delta^{18}O$,‰ vs SMOW) and hydrogen (δD, ‰ vs SMOW) of CO_2, H_2O and H_2 with their contents (mm^3.STP/g). (a) Plot $\delta^{13}C$ vs. $\delta^{18}O$ of CO_2, (b) plot the δD of H_2O vs. $\delta^{18}O$ of CO_2, (c) plot δD of H_2 vs. $\delta^{18}O$ of CO_2, (d) plot δD vs. H_2 contents. Abbreviations as in Fig. 2, MORB from Mattey et al. (1994) and Eiler et al. (1997).

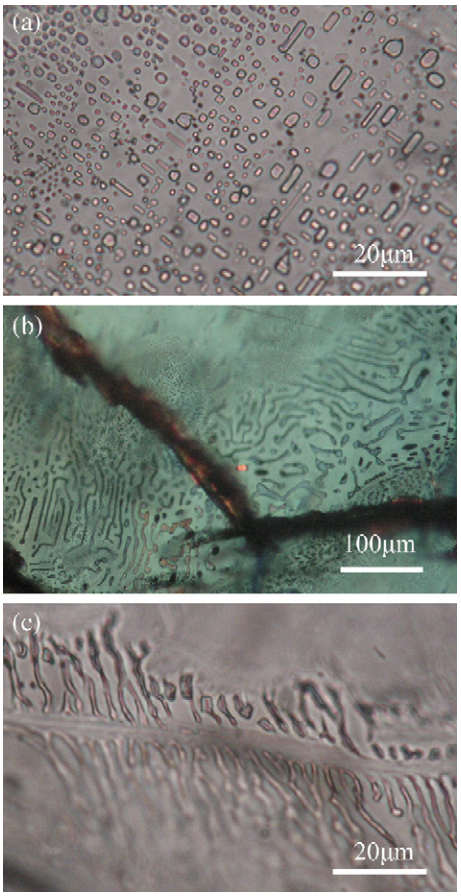


Fig. 6. Photomicrographs of different types of fluid inclusions in the constituent minerals of lherzolite xenoliths. (a) shows early stage fluid inclusions resided in Oliv crystal interiors (sample DF01, single polar) with small size and regular shapes, (b) and (c) show late stage fluid inclusions located at Opx crystal edges (b: sample MP03, crossed polars) and cracks (c: sample DF02, single polar) with large size, irregular shapes, and some micro-cracks developed at edges of these inclusions.

3.4. Volatile types in mantle lherzolite xenoliths

On the basis of releasing temperature, chemical and isotopic composition of volatiles in bulk-rock samples and mineral separates of the lherzolite xenoliths, the following two types of volatiles can be recognized.

Type 1 volatiles released at the 800–1200 °C interval are high in abundance, and are composed of H_2 (~66.64 mm^3.STP/g on average), CO_2 (~50.73) and CO (~35.81). Opx and Cpx have higher concentrations of H_2, CO_2 and CO than Oliv. Type 1 volatiles are characterized isotopically by mantle δD and $\delta^{13}C_{CH4}$ signatures. The δD values of H_2O and H_2 range from −31.1‰ to −96.4‰ with a mean of −64.8‰. The $\delta^{13}C$ of CH_4 become heavier with increasing releasing temperature from 800 °C (a mean of −31.4‰) to 1200 °C (−25.1‰) towards mantle and meteorite compositions (Fig. 3d). The $\delta^{13}C$ values of CO_2 (~−23.6‰ on average) and CO (~−27.3‰) deviate significantly from the mantle values of −5‰ (Deines, 2002), and are significantly lighter than previously documented $\delta^{13}C$ values of ~−5‰ released at >900 °C from xenoliths elsewhere (Pineau and Mathez, 1990; Nadeau et al., 1990).

Type 2 volatiles released at the 400–600 °C interval are low in abundance, and are composed of CO_2 (~9.63 mm^3.STP/g on average) plus CO (~3.27) and H_2 (~1.64). They apparently have $\delta^{13}C$ values of biogenic CH_4 (−56.0‰ to −27.2‰ with a mean of −42.0‰), lighter and variable δD values of H_2O (−110.7‰ to −280.9‰), and variable $\delta^{18}O$ of CO_2 (1.0‰ to 11.5‰). Also, their lighter $\delta^{13}C$ values of CO_2 (~−25.7‰ on average) and CO (~−23.9‰) fall into the fields between oceanic crust and sedimentary organic matters (Fig. 5a).

4. Discussion

4.1. The residence modes of volatiles

The progressive release of CO_2, CO, CH_4 and H_2 with elevated temperatures suggests that these volatiles reside in more than one mode in constituent minerals of the lherzolite xenoliths. Because volatiles possibly absorbed on mineral surfaces and in cracked inclusions are removed by sample pretreatment, and because the rapid trapping of the released volatiles prevents formation of new species (H_2 and CO etc.), the released volatiles are intrinsically stored as fluid inclusions or in crystal structures of the constituent minerals. The constituent minerals of the lherzolite xenoliths have two types of fluid inclusions with melt inclusions, their formation temperatures vary from 987 °C to 1296 °C (Liu et al., 1981; Xia, 1984; Fan and Hooper, 1989; Peng et al., 1994). The early stage fluid inclusions reside in crystal interiors with small size (~0.005–0.02 mm) and regular shapes (Fig. 6a), whereas late stage fluid inclusions are located at crystal edges and healed fractures with large size (~0.01–0.1 mm), irregular shapes, and some micro-cracks developed around these inclusions (Fig. 6b and c).

4.2. The "initial" volatiles in the SCLM beneath eastern China

We define volatiles originally dissolved in mineral structures as "initial" volatiles in the SCLM, and infer that these dissolved volatiles would be trapped in early

stage fluid inclusions when the host rocks and minerals undergo decompression in response to asthenospheric mantle upwelling during early histories of these rocks or under cooling associated with early phases of SCLM development from asthenospheric mantle (Deines, 2002). We further infer that the volatiles in such fluid inclusions may have been well sealed in mineral interiors that survived subsequent mantle events. Type 1 volatiles (see above) may represent such "initial" volatiles in the SCLM, which exhibit typical mantle $\delta^{13}C_{CH4}$ and δD signatures (Figs. 3d and 5b, c). On the other hand, lighter and variable $\delta^{13}C$ and $\delta^{18}O$ of CO_2 and CO relative to previously documented mantle values indicate the involvement of subducted oceanic crust with organic matters of terrigenous sediments (Fig. 5a) (see below).

4.3. Volatiles of metasomatic origin in the SCLM beneath eastern China

Mantle metasomatism is widely observed in the SCLM as indicated by highly depleted major elements (residues of previous melt extraction events) superimposed with elevated abundances of incompatible elements (Zartman et al., 1991; Tatsumoto et al., 1992; Griffin et al., 1998; Zheng et al., 2004). The metasomatism may be macroscopic with metasomatic minerals conspicuous (e.g., amphiboles, phlogopite, apatite etc.) or may be cryptic with the enrichments as hydrous melts distributed along grain boundaries (e.g., O'Reilly and Griffin, 1988). Recrystallization of such metasomatized peridotites would incorporate the metasomatic volatiles as fluid (or melt) inclusions at the edges and healed fractures of the recrystallizing minerals, i.e., late stage fluid inclusions (Peng et al., 1994). Type 2 volatiles may be of such origin. Their formation temperatures are likely to be magmatic at mantle conditions, but their varying releasing temperatures are determined by the physical strength of the crystals around the inclusions, e.g., grain size, inclusion wall thickness, development of cracks (Zhang et al., 2005) etc. Lager size of late stage fluid inclusion with thinner wall thickness, together with the readily developed cracks at their edges, result in their being easily decrepitated. Metasomatic volatiles are characterized by biogenic $\delta^{13}C$ of CH_4, lighter and variable δD of H_2O, lighter $\delta^{13}C$ of CO_2 and CO and variable $\delta^{18}O$ of CO_2 (1.0‰ to 11.5‰) relative to the previously documented values of mantle silicates. The $\delta^{13}C$ values of CH_4 decrease with decreasing releasing temperature towards $\delta^{13}C$ values of biogenic methane (Fig. 3d, Schoell, 1988; Xia and Wang, 1996; Avery and Martens, 1999). Also, the positive $\delta^{13}C$ correlation with CH_4 (Fig. 3c) suggests two components mixing between crustal biogenic origin and mantle origin (Fig. 3d), which can also be inferred from $\delta^{13}C$, $\delta^{18}O$ and δD of the volatile species (Fig. 5a–c).

H_2O in metasomatic volatiles exhibits lighter δD from −110.7‰ to −280.9‰ with a mean of −151.14‰. The δD of H_2 shows lightly positive correlation with $\delta^{18}O$ of CO_2 and negative correlation with H_2 contents (Fig. 5c and d). Ripley et al. (1992) reported that the devolatilization of crustal rocks can produce strong negative δD shift, suggesting that devolatilization of recycled crustal component is likely responsible for lighter δD. Lighter $\delta^{13}C$ and variable $\delta^{18}O$ of CO_2 and CO could be derived from recycled crustal components or sedimentary organic matters (Trull et al., 1993; Deines, 2002; Schulze et al., 2004). The lighter $\delta^{18}O_{CO2}$ values could be derived from subducted altered oceanic crust (Woodhead et al., 1993; Lowry et al., 1999; Macpherson et al., 2000; Widom and Farquhar, 2003; Demeny et al., 2004), and the heavier $\delta^{18}O$ values of CO_2 relative to mantle value (Kyser et al., 1982; Harmon et al., 1986/87; Ionov et al., 1994) are thought to represent altered subducted oceanic crust, recycled terrigenous sediments interacted with low-temperature seawater, mantle degassing or oxygen isotope fractionation among CO_2, CO, H_2O and oxygen in silicate mineral structures (MacGregor and Manton, 1989; Hansteen and Troll, 2003). Therefore, we suggest that metasomatic volatiles are to a large extent determined by a component resembling recycled altered oceanic crust with terrigenous sediments (Figs. 3f and 5a), which may have been incorporated into the recrystallizing Oliv, Opx, and Cpx.

4.4. The recycled crustal components in volatiles

The recycled crustal components are identified in both "initial" volatiles and metasomatic volatiles in the SCLM. The biggest difference between the two recycled crustal components is that the metasomatic volatiles have lighter δD_{H2O} and $\delta^{13}C_{CH4}$ and are enriched CO_2, whereas the "initial" volatiles are dominated by H_2 and have lighter $\delta^{13}C$ of CO_2 and CO and variable $\delta^{18}O$ of CO_2, which are interpreted as subducted oceanic crust with terrigenous sediments in active (convergent) continental margin with large terrigenous weathering.

The recycled crustal components in metasomatic volatiles are interpreted as the devolatilization of altered oceanic crust with terrigenous sediments; the recycled altered oceanic crustal fluids are likely involved in

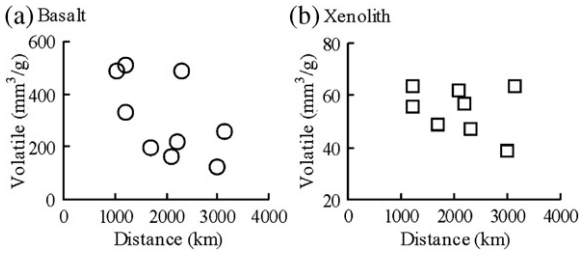


Fig. 7. Plots of volatile abundances (mm^3.STP/g) of Cenozoic alkali basalts (a) and lherzolite xenoliths (b) with the latitudinal distance from sample localities to subduction zone of Pacific plate. The distance refers to the latitudinal distance from subduction zone of Pacific plate to sample localities.

SCLM beneath eastern China during two metasomatism events identified by Sr, Nd and Pb isotopic data of the xenoliths (Zartman et al., 1991; Griffin et al., 1998; Zheng et al., 2004). The dehydration of subducted paleo-Pacific (or predecessor) oceanic lithosphere (Niu, 2005) that is presently lying horizontally in the transition zone beneath eastern Chinese continent, as shown by seismic tomography (Karason and van der Hilst, 2000; Ai et al., 2003; Li and Yuan, 2003), favors this interpretation. Niu (2005) suggested the Mesozoic lithosphere thinning in eastern China may have resulted from a process that "transformed" the deep portion of the lithosphere into convective asthenosphere by hydration-weakening, and the water that did so may come from dehydration of subducted Pacific (or predecessor) oceanic lithosphere that lies horizontally in the transition zone beneath eastern China (Niu et al., 2003; Niu, 2004, 2005). This hypothesis is supported by abundance changes of volatiles in Cenozoic alkali basalts and hosted lherzolite xenoliths (Zhang et al., 1999) and variable $\delta^{18}O$ of CO_2 and lighter δD of H_2O in metasomatic volatiles. The volatile abundances in alkali basalts and lherzolite xenoliths increase with decreasing latitudinal distances from the localities of alkali basalts and lherzolite xenolith to the subduction zone of paleo- and present-day western Pacific plate (Fig. 7), i.e. volatile abundances increase progressively from northern localities to southern localities. On the other hand, variable $\delta^{18}O$ of CO_2 and lighter δD of H_2O suggest the degassing of subducted altered oceanic crust as recorded in the SCLM of eastern China. That was also supported by the EMII signature of Sr, Nd and Pb isotopes of mantle xenoliths in eastern China, which may be introduced by a metasomatic event during the subduction of an oceanic plate (Tatsumoto et al., 1992). It follows that the dehydration of altered and subducted Pacific (or predecessor) oceanic lithosphere can very well explain the overall characteristics of volatiles of mantle metasomatism revealed through lherzolite xenoliths presented in this study.

5. Conclusion

The concentrations and C–O–H isotopic compositions of CO_2, CO, CH_4, H_2O and H_2 volatile species preserved in lherzolite xenoliths from eastern China provide insights into the origin of the volatiles and also some new perspectives on the evolution of SCLM in the region. The main conclusions are:

(1) two types of volatiles are recognized in lherzolite xenoliths from eastern China. They include 1) "initial" volatiles in the SCLM which are originally retained in mineral structures, but trapped during SCLM evolution as early stage fluid inclusions preserved in the interiors of Oliv, Opx and Cpx crystals and released at 800–1200 °C interval, and 2) metasomatic volatiles, which were incorporated into late stage fluid inclusions at the edges and healed fractures of the recrystallizing crystals during mantle metasomatism, and released at lower temperatures of 400 °C to 600 °C because of larger size and cracks of late stage fluid inclusions.
(2) "initial" volatiles dominated by H_2 are a mixture between normal mantle volatiles with typical mantle δD and $\delta^{13}C_{CH4}$ signatures of H_2, H_2O and CH_4 and recycled crustal volatiles. The recycled crustal volatiles have lighter $\delta^{13}C$ of CO_2, CO, variable $\delta^{18}O$ and could have been derived from subducted oceanic crust with terrigenous sediments in an active (convergent) continental margin.
(3) metasomatic volatiles composed of CO_2 are the recycled crustal volatiles of oceanic origin (e.g., the devolatilization of altered oceanic crust) with continental origin (e.g., terrigenous sediments), which may have derived from dehydration of the subducted paleo-Pacific lithosphere that lies horizontally in the transition zone beneath eastern China. Such recycled crustal fluids may be an important agent that has metasomatized SCLM beneath eastern China and may have played a critical role in the process of lithosphere thinning in the Mesozoic.

Acknowledgements

This study was supported by grants from NSFC (40273009), NCET and State Key Lab of Gas-Geochemistry, Institute of Geology and Geophysics, CAS. We thank Liwu Li and Qibin Wen for analytical assistance, W. L. Griffin for discussion, Zhengfu Guo

and Ed Ripley for critical and constructive reviews, and Steve Foley for editorial effort.

Reference

Ai, Y.-S., Zheng, T.-Y., Xu, W.-W., He, Y.-M., Dong, D., 2003. A complex 660 km discontinuity beneath northeast China. Earth and Planetary Science Letters 212, 63–71.

Avery Jr., G.B., Martens, C.S., 1999. Controls on the stable carbon isotopic composition of biogenic methane produced in a tidal freshwater estaurine sediment. Geochimica et Cosmochimica Acta 63, 1075–1082.

Boettcher, A.L., O'Neil, J.R., 1980. Stable isotope, chemical, and petrographic studies of high-pressure amphiboles and micas: evidence for metasomatism in the mantle source regions of alkali basalts and kimberlites. American Journal of Science 280-A, 594–621.

Brady, J.B., 1995. Diffusion data for silicate minerals, glasses, and liquids. In: Ahrens, T.J. (Ed.), Mineral physics and cystallography: a handbook of physical constants. The American Geophysical Union, Washington, Reference Shelf, vol. 2, pp. 269–290.

Deines, P., 2002. The carbon isotope geochemistry of mantle xenoliths. Earth-Science Reviews 58, 247–278.

Deines, P., Harris, J.W., Gurney, J.J., 1997. Carbon isotope ratios, nitrogen content and aggregation state, and inclusion chemistry of diamonds from Jwaneng, Botswana. Geochimica et Cosmochimica Acta 61, 3993–4005.

Demeny, A., Vennemann, T.W., Hegner, E., Ahijado, A., Casillas, R., Nagy, G., Homonnay, Z., Gutierrez, M., Szabo, Cs., 2004. H, O, Sr, Nd, and Pb isotopic evidence for recycled oceanic crust in the Transitional Volcanic Group of Fuerteventura, Canary Islands, Spain. Chemical Geology 205, 37–54.

Eiler, J.M., Farley, K.A., Valley, J.W., Stolper, E.M., Hauri, E.H., Craig, H., 1995. Oxygen isotope evidence against bulk recycled sediment in the mantle sources of Pitcairn Island lavas. Nature 377, 138–141.

Eiler, J.M., Farley, K.A., Valley, J.W., Hofmann, A.W., Stolper, E.M., 1996. Oxygen isotope constraints on the sources of Hawaiian volcanism. Earth and Planetary Science Letters 144, 453–468.

Eiler, J.M., Farley, K.A., Valley, J.W., Hauri, E., Craig, H., Hart, S.R., Stolper, E.M., 1997. Oxygen isotope variations in ocean island basalt phenocrysts. Geochimica et Cosmochimica Acta 61, 2281–2293.

Exley, R.A., Mattey, K.P., Clague, K.A., Pillinger, C.T., 1986. Carbon isotope systematics of a mantle "hot spot": a comparison of Loihi Seamount and MORB glasses. Earth and Planetary Science Letters 78, 189–199.

Fan, Q.-C., Hooper, P.R., 1989. The mineral chemistry of ultramafic xenoliths of eastern China: Implications for upper mantle composition and the palaeogeotherms. Journal of Petrology 30, 1117–1158.

Griffin, W.L., Zhang, A., O'Reilly, S.Y., Ryan, C.G., 1998. Phanerozoic evolution of the lithosphere beneath the Sino-Korean craton. In: Flower, M., Chung, S.L., Lo, C.H., Lee, Y.Y. (Eds.), Mantle dynamics and plate interactions in east Asia. Am. Geodynamics Series, vol. 27. American Geophysical Union, Washington, DC, pp. 107–126.

Hansteen, T.H., Troll, V.R., 2003. Oxygen isotope composition of xenoliths from the oceanic crust and volcanic edifice beneath Gran Canaria (Canary Islands). Chemical Geology 193, 181–193.

Harmon, R.S., Hoefs, J., 1995. Oxygen isotope heterogeneity of the mantle deduced from global $\delta^{18}O$ systematics of basalts from different geotectonic settings. Contributions to Mineralogy and Petrology 120, 95–114.

Harmon, R.S., Kempton, P.D., Stosch, H.G., Hoefs, J., Kovalenko, V.I., Ionov, D., 1986/87. $^{18}O/^{16}O$ ratios in anhydrous spinel lherzolite xenoliths from the Shavaryn-Tsaram volcano, Mongolia. Earth and Planetary Science Letters 81, 193–202.

Ionov, D.A., Harmon, R.S., France-Lanord, C., Greenwood, P.B., Ashchepkov, I.V., 1994. Oxygen isotope composition of garnet and spinel peridotites in the continental mantle: evidence from the Vitim xenolith suite, southern Siberia. Geochimica et Cosmochimica Acta 58, 1463–1470.

Karason, H., van der Hilst, R., 2000. Constraints on mantle convection from seismic tomography. Geophysical Monograph 121, 277–288.

Kelley, D.S., Frueh-Green, G., 1995. Methane concentrations and isotopic compositions in layer 3 of the oceanic crust. EOS 76, F675.

Konnerup-Madsen, J., Kreulen, R., Rose-Hansen, J., 1988. Stable isotope characteristics of hydrocarbon gases in alkaline Ilimaussq complex, south Greenland. Bulletin of Mineralogy 111, 567–576.

Kyser, T.K., 1986. Stable isotope variations in the mantle. In: Valley, J.W., TaylorJr. Jr., H.P., O'Neil, J.R. (Eds.), Stable isotopes in high temperature geological processes. . Reviews in Mineralogy, vol. 16. Mineralogical Society of America, Washington DC, USA, pp. 141–164.

Kyser, T.K., O'Neil, J.R., 1984. Hydrogen isotope systematics of submarine basalts. Geochimica et Cosmochimica Acta 48, 2123–2133.

Kyser, T.K., O'Neil, J.R., Carmichael, I.S.E., 1982. Genetic relations among basic lavas and ultramafic nodules: evidence from oxygen isotope compositions. Contributions to Mineralogy and Petrology 81, 88–102.

Li, X.-Q., Yuan, X.-H., 2003. Receiver functions in northeast China: implications for slab penetration into the lower mantle in northwest Pacific subduction zone. Earth and Planetary Science Letters 216, 679–691.

Liu, R.-X., Yang, M.-E., Xu, H.-J., 1981. Preliminary study on ultra-mafic xenoliths of alkali basalts in Northeastern China. Seismological Geology Sinica 3, 1–16 (in Chinese with English abstract).

Lowry, D., Mattey, D.P., Harris, J.W., 1999. Oxygen isotope composition of syngenetic inclusions in diamond from the Finsch Mine, RSA. Geochimica et Cosmochimica Acta 63, 1825–1836.

MacGregor, I.D., Manton, W.I., 1989. Roberts Victor eclogites: ancient oceanic crust. Journal of Geophysical Research 91, 14063–14079.

Macpherson, C.G., Hilton, D.R., Mattey, D.P., Sinton, J.M., 2000. Evidence for an ^{18}O-depleted mantle plume from contrasting $^{18}O/^{16}O$ ratios of back-arc lavas from the Manus Basin and Mariana Trough. Earth and Planetary Science Letters 176, 171–183.

Mattey, D.P., Exley, R.A., Pillinger, C.T., 1984. Isotope composition of CO_2 and dissolved carbon species in basalt glass. Geochimica et Cosmochimica Acta 52, 2377–2386.

Mattey, D., Lowry, D., Macpheson, C., 1994. Oxygen isotope composition of mantle peridotite. Earth and Planetary Science Letters 128, 231–241.

Nadeau, S., Pineau, F., Javoy, M., 1990. Carbon concentrations and isotopic ratios in fluid-inclusion-bearing upper-mantle xenoliths along the northwestern margin of North America. Chemical Geology 81, 271–297.

Niu, Y., 2004. Bulk-rock major and trace element compositions of abyssal peridotites: Implications for mantle melting, melt extraction and post-melting processes beneath ocean ridges. Journal of Petrology 45, 2423–2458.

Niu, Y., 2005. Generation and evolution of basaltic magmas: Some basic concepts and a new view on the origin of Mesozoic–Cenozoic basaltic volcanism in eastern China. Geological Journal of China Universities 11, 9–46.

Niu, Y., O'Hara, M.J., Pearce, J.A., 2003. Initiation of subduction zones as a consequence of lateral compositional buoyancy contrast within the lithosphere: a petrologic perspective. Journal of Petrology 44, 851–866.

O'Reilly, S.Y., Griffin, W.L., 1988. Mantle metasomatism beneath western Victoria, Australia: I, Metasomatic processes in Cr-diopside lherzolites. Geochimica et Cosmochimica Acta 52, 433–447.

Peng, L.-G., Liu, R.-X., Fan, Q.-C., 1994. Fluid and melt inclusion releases of pyrolite xenoliths from the shore of southern China. Acta Petrologica Sinica 10, 440–448 (in Chinese with English abstract).

Pineau, F., Mathez, E.A., 1990. Carbon isotopes in xenoliths from the Hualalai volcano, Hawaii, and the generation of isotopic variability. Geochimica et Cosmochimica Acta 54, 217–227.

Ripley, E.M., Butler, B.K., Taib, N.I., 1992. Effects of devolatilization on the hydrogen isotopic composition of pelitic rocks in the contact aureole of the Duluth Complex, northeastern Minnesota, U.S.A. Chemical Geology 102, 185–197.

Schoell, M., 1988. Multiple origins of methane in the Earth. Chemical Geology 71, 1–10.

Schulze, D.J., Harte, B., Valley, J.W., Channer, D.M., 2004. Evidence of subduction and crust-mantle mixing from a single diamond. Lithos 77, 349–358.

Shaw, A.M., Hilton, D.R., Macpherson, C.G., Sinton, J.M., 2004. The CO_2-He-Ar-H_2O systematics of the Manus back-arc basin: resolving source composition from degassing and contamination effects. Geochimica et Cosmochimica Acta 68, 1837–1856.

Tatsumoto, M., Basu, A.R., Huang, W.K., 1992. Sr, Nd, and Pb isotopes of ultramafic xenoliths in volcanic rock of eastern China: enriched components EMI and EMII in subcontinental lithosphere. Earth and Planetary Science Letters 113, 107–128.

Taylor, B.E., 1986. Magmatic volatiles: isotopic variation of C, H, and S. In: Valley, J.W. (Ed.), Stable isotopes in high temperature geological processes. Mineralogical Society of America, vol. 16, pp. 185–225.

Trull, T., Nadean, S., Pineau, F., Polve, M., Javoy, M., 1993. C-He systematics in hotspot xenoliths: Implications for mantle carbon contents and carbon recycling. Earth and Planetary Science Letters 118, 43–64.

Widom, E., Farquhar, J., 2003. Oxygen isotope signatures in olivines from Sao Miguel (Azores) basalts: implications for crustal and mantle processes. Chemical Geology 193, 237–255.

Woodhead, J.D., Greenwood, P., Harmon, R.S., Stoffers, P., 1993. Oxygen isotope evidence for recycled crust in the source of EM type ocean island basalts. Nature 362, 809–813.

Xia, L.Q., 1984. Highly dense CO_2 fluid inclusions in peridotitic inclusions in some alkali-basalts from east China. Acta Mineralogica Sinica 4, 133–142 (in Chinese with English abstract).

Xia, X.Y., Wang, X.B., 1996. The concentration and carbon isotopes of hydrocarbons resolved in upper water of western Pacific Ocean. Acta Sedimentologica Sinica 14, 45–49 (in Chinese with English abstract).

Xia, Q., Dallai, L., Deloule, E., 2004. Oxygen and hydrogen isotope heterogeneity of clinopyroxene megacrysts from Nushan Volcano, SE China. Chemical Geology 209, 137–151.

Yuen, G., Blair, N., Des Marais, D.J., Chang, S., 1984. Carbon isotope composition of low molecular weight hydrocarbons and monocarboxylic acids from Murchison meteorite. Nature 307, 252–254.

Zartman, R.E., Futa, K., Peng, Z.C., 1991. A comparison of Sr-Nd-Pb isotopes in young and old continental lithospheric mantle: Patagonia and eastern China. Australian Journal of Earth Sciences 38, 545–547.

Zhang, M.-J., Wang, X.-B., Liu, G., Li, L.-W., 1999. The volatile compositions of the fluids in alkali-basalts and mantle-derived xenoliths in Eastern China. Acta Geologica Sinica 73, 162–166 (in Chinese with English abstract).

Zhang, M.-J., Wang, X.-B., Liu, G., Zhang, T.-W., Bo, W.-R., 2004. The compositions of upper mantle fluids beneath Eastern China: implications for mantle evolution. Acta Geologica Sinica 78, 125–130.

Zhang, M.-J., Hu, P.-Q., Zheng, P., Wang, X.-B., Li, L.-W., 2005. The occurrence modes of H_2 in mantle-derived rocks. In: Mao, J., Bierlein, F.P. (Eds.), Mineral deposit research. Springer, New York, pp. 73–76.

Zheng, J.-P., O'Reilly, S.Y., Griffin, W.L., Zhang, M., Lu, F.-X., Liu, G.-L., 2004. Nature and evolution of Mesozoic-Cenozoic lithospheric mantle beneath the Cathaysia block, SE China. Lithos 74, 41–65.